MATERIALS PHYSICS AND MECHANICS RESEARCH ARTICLE

Submitted: October 3, 2025 **Revised: November 7, 2025** **Accepted: November 17, 2025**

Rayleigh waves in a rotating inhomogeneous half-space with magnetic effect under impedance and variable amplitudes of corrugation

A.I. Anya

Veritas University, Abuja, Bwari-Abuja, Nigeria

anyaa@veritas.edu.ng

ABSTRACT

A mathematical model investigating the dispersions of Rayleigh wave on an inhomogeneous rotating half-space with magnetic field influence, impedance and variable amplitudes of corrugation is presented. Normal mode approach and non-dimensionalization principles were employed to the equations of motion. Derivations of the analytical solutions of the stresses and displacement components occasioned by the wave on the material were achieved. Variable amplitudes of corrugation due to a linear function incorporated as the amplitude of the trigonometric Fourier series and the impedance conditions enriches the material characterizations and paved way in formulating the structure or nature of corrugation at the boundary. Thus, dispersion relations of Rayleigh waves due to homogeneous impedance and inhomogeneous impedance were analytically given and graphically depicted with the variations of the physical parameters.

KEYWORDS

variable amplitude of corrugation • inhomogeneous fiber-reinforcement • magnetism • rotation of the medium homogeneous and inhomogeneous impedance boundaries • dispersion of Rayleigh wave

Citation: Anya AI. Rayleigh waves in a rotating inhomogeneous half-space with magnetic effect under impedance and variable amplitudes of corrugation. *Materials Physics and Mechanics*. 2025;53(6): 164–181. http://dx.doi.org/10.18149/MPM.5362025_12

Introduction

Mechanical wave propagation is dependent on the physical composition of materials. Scientists in the fields of seismology and geophysical analysis usually devote and maintain clear position in examining compositions associated with most materials before employing them into structural and engineering constructions or applications. This is largely pertinent to ensure quality occasioned by such materials through which waves and in particular surface waves modulate. These materials are classed into two forms; anisotropic and isotropic materials and following which homogeneous and inhomogeneous characterization of the materials would ensue. Also, the inhomogeneity of these materials hugely depends on the nature of the deformation which typically lies in the form of growth or decay of the material parameters or other geometrical considerations of the interacting material constants.

Furthermore, mathematics, physics, and geophysics scientists have maintained constant researches in this field of solid mechanics by exploring and developing models that could necessitate great insights about the behaviors of these materials when acted upon by stress and other environmental factors. Given this, the consideration of just isotropic material may not holistically define or describe exact continuum information in composites. Part of

Publisher: Peter the Great St. Petersburg Polytechnic University

this line of thought yielded examination on anisotropic material exhibitions. Anisotropic materials exist as composites, for instance, the Fiber-reinforced composites, and the orthotropic materials, etc., to mention but a few, are highly regarded for engineering applications due to their high positive mechanical properties. On this note, Spencer [1] developed and presented a work that hinged on deformation of fiber-reinforced material as a composite whose characterizations in terms of tensile strength, weightlessness (leading to flexibility), and so on, endears them to various industrial applications.

In a different vein, fiber-reinforced composites, also, might not give definite results in terms of its behavior if the environmental factors or other physical interacting quantities like magnetic fields Abd-Alla et al. [2] or maybe rotation Schoenberg et al. [3] surrounding it are not factored into the mathematical model equations characterizing a particular phenomenon. This is solely because they have a way of giving near accurate predictions of the model problem needed for insightful reach of decisions. Aside the surrounding characterizations, researchers equally exploit other mechanical properties such as the impedance [4], which act like a resistance to the motion of matter or acoustic energy on a material alongside appropriate boundary conditions which could be planar or non-planar like the corrugated boundary [5] to enrich the understating of some complex mechanical structures and surface wave (Stoneley wave, Love wave and Rayleigh wave) propagations along and across interfaces of materials. Hence, the basic mechanical reasoning behind this design of corrugation is to positively enhance the stiffness-to-weight ratio of the material by giving optimal geometric representation rather than addition of more material. Thus, increase in bending stiffness, energy absorption, and anisotropic behavior exhibitions cum buckling resistance are some of the key principles behind corrugation of materials. While variable corrugation shapes or geometries of different heights, or even hierarchical construction on materials, allows for further enhancement and optimization of the mechanical properties of the material for a particular performance needs.

In the foregoing, several authors have made contributions to further the investigations associated with these corrugated-impedance boundary effects on materials along with other interesting wave phenomena. Singh et al. [6] and Singh et al. [7,8] worked on qP-wave at a corrugated interface between two different initial stress elastic semi-infinite material, influence of corrugated boundary surfaces reinforcement, hydrostatic stress, heterogeneity and anisotropy on Love type wave propagation and also on the effect of loose bonding and corrugation on Rayleigh-type wave modulation. More so, Das et al. [9] dealt with surface waves in an inhomogeneous material which included gravity. Abd-Alla et al. [10] investigated impact of rotation on a non-homogeneous infinite elastic cylinder of orthotropic material under magnetic influences. Chattopadhyay et al. [11] opined the dispersion equation of Love wave based on irregularity in the thickness of non-homogeneous crustal layer. Following this trend, Roy et al. [12] worked on the propagation and reflection of plane waves in a rotating magneto-elastic fiber-reinforced semi space with surface stress. Singh et al. [13], Gupta et al. [14], Anya et al. [15–18] dealt on magnetic effects on surface waves in a rotating non-homogeneous half-space with grooved-impedance boundary conditions and non-local effects, respectively. Likewise, Maleki et al. [19] developed model tests on determining the effect of various geometrical aspects on horizontal impedance function of

surface footings. Chowdhury et al. [20] examined the dispersion of Stoneley waves through the irregular common interface of two hydrostatic stressed MTI media. Singh et al. [21,22] contributed their investigation on Rayleigh wave at an impedance boundary of an incompressible micropolar and orthotropic solid, respectively while Sahu et al. [23] dealt on the Mathematical analysis of Rayleigh waves at the imperfect boundary between orthotropic and micropolar media. Giovannini [24] worked on the theory of dipole-exchange spin-wave propagation in periodically corrugated films. And Rakshit et al. [25,26] also proposed a stress analysis for the irregular surface of visco-porous piezoelectric half-space subjected to a moving load. Subsequently, Gupta et al. [27] presented different theories of thermo-elasticity under the Rayleigh wave propagation along an isothermal boundary while Kaushal et al. [28] examined wave propagation under the influence of voids and non-free surfaces in a micropolar elastic medium. Also, Sharma et al. [29] dealt on the fractional strain analysis on reflection of plane waves at an impedance boundary of non-local swelling porous thermo-elastic medium. Sharma et al. [30] further made input on the effect of rotation for generalized thermo-viscoelastic Rayleigh-Lamb wave propagating on materials while its counterpart Shaw et al. [31] utilized eigen function expansion approach to examine Rayleigh wave propagation in an orthotropic magneto-thermoelastic half-space. Moreover, Othman et al. [32–34] incorporated effects of magnetic field on a rotating thermo-elastic medium with some other physical properties like voids, relaxation time and reinforcement of fibers to study wave propagation on structures. Thus, we observed keenly that all these investigations were associated with singular or part investigations of the interacting physical quantities of rotation, micropolar effects, homogeneity, inhomogeneity, magnetism, corrugation, etc., which fall short as constituted in this present investigation where the corrugation effects possess variable amplitudes whilst considering different ideas of impedance characterizations in generating the dispersions of Rayleigh wave.

In view of the literatures posited above, the present investigation is geared towards exploring a mathematical model and analysis on the dispersion of Rayleigh wave for a rotating inhomogeneous fiber-reinforced solid with magnetic influences under impedance and variable amplitudes of corrugation. Following this, the variable amplitude of corrugation is conceived to be a linear function of the horizontal coordinate and incorporated at the point of the constant amplitude using the Trigonometric Fourier series cosine terms. The equations of motion were derived using the stress-strain relations of a fiber-reinforced material through the fundamental governing laws of motion of Physics. In addition, the analytical solution is developed by utilizing the eigenvalue method also called normal mode method. We developed both the homogeneous and inhomogeneous impedance conditions at the boundary via which the two dispersion relations of the Rayleigh wave were analytically derived and presented. Graphical results depicting the impact of the contributing physical parameters of inhomogeneity, rotation of the medium, corrugation parameters (variable amplitude parameters), wavenumber, and magnetic effect on the two dispersion relations of the Rayleigh wave due to homogeneous and inhomogeneous impedance were achieved. We observe that particular cases found in the literature can be obtained from our results as special cases especially when we neglect one of the parameters associated with the variable amplitudes of corrugation leading to constant or uniform amplitude of corrugation model.

The mathematical model and formulations

In this section, we introduce the basic fields' equations characterizing the mathematical model. In line with this, the mathematical formulations of the model using the constitutive equations of fiber-reinforced material in its homogeneous form as introduced by Spencer [1] and the magnetic field effect, Abd-Alla et al. [2] and Anya et al. [35,36] are given below:

$$\sigma_{ij} = \lambda\varepsilon_{kk}\delta_{ij} + 2\mu_T\varepsilon_{ij} + \alpha\left(f_k f_m \varepsilon_{km}\delta_{ij} + \varepsilon_{kk} f_i f_j\right) + 2(\mu_L - \mu_T)\left(f_i f_k \varepsilon_{kj} + \right.$$
$$\left. + f_j f_k \varepsilon_{ki}\right) + \beta\left(f_k f_m \varepsilon_{km} f_i f_j\right), i = j = k = m = 1,2,3, \quad (1)$$

$$F_i = \mu_0 H_0^2\left(e_{,1} - \varepsilon_0\mu_0\ddot{u}_1, e_{,2} - \varepsilon_0\mu_0\ddot{u}_2, 0\right),\ i = 1,2,3, \quad (2)$$

where σ_{ij} denotes the stress tensor, ε_{ij} prescribe the strain tensor, u_i represents the displacement vector, λ stipulate the Lames constant, $(\alpha, \beta, (\mu_L - \mu_T))$ are the fiber-reinforced parameters, δ_{ij} entails the Kronecker-delta function; and F_i implies the magnetic force such that $F_i = (F_1, F_2, F_3)$. However, the strain is equally defined to be mathematically represented as $\varepsilon_{ij} = \frac{1}{2}\left(u_{i,j} + u_{j,i}\right)$ and $f = (f_1, f_2, f_3)$ such that $f = (1,0,0)$ prescribe the fiber-reinforced directions. H_i is the magnetic vector field defined to be $H_i = H_0\delta_{i3} + h_i$, $h_i = (0,0,-e)$, $e = u_{i,i}$, $i = 1,2$. Also, h_i is induced magnetic field such that ε_0 and μ_0 connotes the electric permeability and the magnetic permeability, as the case maybe, owing to the Maxwell's theory of electromagnetism. This model postulates its analysis in 2-D such that x_1x_2-plane becomes the plane of consideration and such that $h_i(x_1, x_2, x_3) = -u_{k,k}\delta_{i3}$. Owing to all these formulations, the governing equations of motion for the rotating Schoenberg et al. [3] homogeneous fiber-reinforced material under magnetic field are thus, presented:

$$\sigma_{ij,j} + F_i = \rho\{\ddot{u}_i + \Omega_j u_j \Omega_i - \Omega^2 u_i - 2\varepsilon_{ijk}\Omega_j\dot{u}_k\}. \quad (3)$$

The parameters in Eq. (3) like the ε_{jim} represents the Levi-Civita tensor (alternating symbol) and Ω stipulates the rotation of the medium. Einstein summation indices are used and where index after comma represents partial rate of change with respect to coordinate and superscript dot stipulate partial rate of change with respect to time. Since our formulation is making use of the deformation in the x_1x_2-plane, we take $x_3 = 0$ and $\Omega(0,0,1)$ as the rotation (which purely involved the Coriolis and centrifugal forces arising from a rotating coordinate frame) of the half-space about the x_3-axis. It then means that the displacements $u_1 \neq 0$ and $u_2 \neq 0$, for any change in plane and coordiantes of consideration.

Furthermore, the material is originally presumed to be inhomogeneous but the fiber-reinforced medium so presented in Eq. (1) is homogeneous. It suffices that the parameters of the homogeneous fiber-reinforced material be considered to decay or grow such that the rate of the occurrence is proportional to its value at that instance. This would ultimately introduce the inhomogeneity into the model. This is such that the elastic module, elastic parameters, and density of the half-space take the representation: $(\lambda, \alpha, \mu_L, \mu_T, \beta, \rho) = (\lambda_0, \alpha_0, \mu_{L0}, \mu_{T_0}, \beta_0, \rho_0)e^{-mx_2}$, Khan et al. [37] and Munish et al. [38]. In the given proportionality above, m describes the inhomogeneity of the fiber-reinforced material.

Thus, employing these inhomogeneous parameters into Eq. (1), the component forms of the equations of motion of the wave are presented:

$$(\lambda + 2\alpha + 4\mu_L - 2\mu_T + \beta + \mu_0 H_0^2)u_{1,11} + (\alpha + \lambda + \mu_L + \mu_0 H_0^2)u_{2,21} + \mu_L u_{1,22} - -m\mu_T(u_{1,2} + u_{2,1}) = \{\rho + \varepsilon_0\mu_0^2 H_0^2\}\ddot{u}_1 - \rho\Omega^2 u_1 - 2\Omega\dot{u}_2\}, \quad (4)$$

$$(\alpha + \lambda + \mu_L + \mu_0 H_0^2)u_{1,12} + \mu_L u_{2,11} + (\lambda + 2\mu_T + \mu_0 H_0^2)u_{2,22} - m(\lambda + \alpha)u_{1,1} - -m(\lambda + 2\mu_T)u_{2,2} = \{\rho + \varepsilon_0\mu_0^2 H_0^2\}\ddot{u}_2 - \rho\{\Omega^2 u_2 + 2\Omega\dot{u}_1\}, \quad (5)$$

$$\mu_L u_{3,11} + \mu_T u_{3,22} - m\mu_T u_{3,2} = \rho\ddot{u}_3. \quad (6)$$

We can restructure Eqs. (4)–(6) as follows:

$$G_1 u_{1,11} + G_2 u_{2,21} + G_3 u_{1,22} - mG_4(u_{1,2} + u_{2,1}) = \{\{\rho + \varepsilon_0\mu_0^2 H_0^2\}\ddot{u}_1 - \rho(\Omega^2 u_1 + 2\Omega\dot{u}_2)\}, \quad (7)$$

$$G_2 u_{1,12} + G_3 u_{2,11} + G_5 u_{2,22} - mG_6 u_{1,1} - mG_7 u_{2,2} = \{\{\rho + \varepsilon_0\mu_0^2 H_0^2\}\ddot{u}_2 - \rho(\Omega^2 u_2 - 2\Omega\dot{u}_1)\}, \quad (8)$$

$$G_3 u_{3,11} + G_4 u_{3,22} - mG_4 u_{3,2} = \rho\ddot{u}_3, \quad (9)$$

where $G_1 = (\lambda + 2\alpha + 4\mu_L - 2\mu_T + \beta + \mu_0 H_0^2)$, $G_2 = (\alpha + \lambda + \mu_L + \mu_0 H_0^2)$, $G_3 = \mu_L$, $G_4 = \mu_T$, $G_5 = (\lambda + 2\mu_T + \mu_0 H_0^2)$, $G_6 = (\lambda + \alpha)$, $G_7 = (\lambda + 2\mu_T)$.

If we employ $m = 0$ into Eqs. (7)–(9), the homogeneous material characterizing the equations of the wave motion is recovered. In addition, let us define the following dimensionless variables: $(x_1', x_2', u_1', u_2') = c_0(x_1, x_2, u_1, u_2)$, $c_0^2, = G_1/\rho, (t') = c_0^2 t$, $\Omega' = \Omega/c_0^2$, $\sigma_{ij}' = \sigma_{ij}/\rho c_0^2$, and employ them into Eqs. (7)–(9). Dropping the sign " ′" from the equations results to the dimensionless form of the equations of the wave motion below:

$$u_{1,11} + G_{12}u_{2,21} + G_{13}u_{1,22} - mG_{24}(u_{1,2} + u_{2,1}) = \left\{\left\{1 + \frac{\varepsilon_0\mu_0^2 H_0^2}{\rho}\right\}\ddot{u}_1 - \rho\Omega^2 u_1 - 2\rho\Omega\dot{u}_2\right\} \quad (10)$$

$$G_{12}u_{1,12} + G_{13}u_{2,11} + G_{15}u_{2,22} - mG_{26}u_{1,1} - mG_{27}u_{2,2} = \{\{1 + \varepsilon_0\mu_0^2 H_0^2/\rho\}\ddot{u}_2 - \rho\Omega^2 u_2 + 2\rho\Omega\dot{u}_1\}, \quad (11)$$

$$G_{13}u_{3,11} + G_{14}u_{3,22} - mG_{24}u_{3,2} = \ddot{u}_3,$$

$$(G_{12}, G_{13}, G_{14}, G_{15}, G_{16}, B_{17}) = ((G_2, G_3, G_4, G_5, G_6, G_7)/G_1), \quad (12)$$

$$(G_{24}, G_{26}, G_{27}) = (G_{14}, G_{16}, G_{17})\rho^{1/2}/G_1^{3/2}.$$

Analytical solution of the problem and normal mode analysis

This section employs the eigenvalue approach also called the normal mode solution approach in the derivation of the analytical solutions of the displacement components and subsequently, the normal and shear stresses on the rotating inhomogeneous impedance-corrugated fiber-reinforced solid. Thus, adopting the fact that this approach of normal mode analysis be applicable, the waves have their displacement components as:

$$u_i = (\hat{u}_i(x_2))e^{\omega t + ibx_1};\ i = 1,2. \quad (13)$$

Employing Eq. (13) into Eqs. (10)–(12), three ordinary differential equations (ODEs) in the x_2 coordinates are given:

$$(G_{13}D^2 - mG_{24}D - b^2 - g1)\hat{u}_1 + (iG_{12}bD - mG_{24}bi - 2\rho\Omega\omega)\hat{u}_2 = 0, \quad (14)$$

$$(iG_{12}bD - mbiG_{26} + 2\rho\Omega\omega)\hat{u}_1 + (G_{15}D^2 - mG_{27}D - G_{13}b^2 - g1)\hat{u}_2 = 0, \quad (15)$$

$$(G_{14}D^2 - mG_{24}D - (G_{13}b^2 + \rho\omega^2)\hat{u}_3 = 0. \quad (16)$$

In Eqs. (14)–(15), $g1 = (1 + \varepsilon_0\mu_0^2 H_0^2/\rho)\omega^2 + \rho\Omega^2)$. Note that D^2 entails second order ordinary derivative with respect to x_2. For non-trivial solution, Eqs. (14)–(15) produce 4th order ordinary differential equation below where $\hat{u}_1, \hat{u}_2$ becomes the dependent variables and x_2 the independent variable. That is, the determinant of the coefficients of $\hat{u}_1, \hat{u}_2$ are equated to zero whereas $(\hat{u}_1, \hat{u}_2) \neq 0$. Observe that Eq. (16) is

uncoupled with Eqs. (14)–(15) and thus, we neglect it from forming the associated characteristic equation below. This is because we based our analysis in a plane geometry. However, its solution can be easily obtained by using quadratic formula:

$$(d_{11}D^4 + d_{12}D^3 + d_{13}D^2 + d_{14}D + d_{15})(\hat{u}_1, \hat{u}_2) = 0, \tag{17}$$

where $d_{1i}, i = 1,2,3,4,5$ are complex coefficients which depends on the parameters of the solid half-space. Assume that $\eta_i, i = 1,2,3,4$ be positive roots of Eq. (17), thus, the normal mode analysis gives the solutions of $\hat{u}_1, \hat{u}_2$ as follows:

$$(\hat{u}_1, \hat{u}_2) = (K_n, K_{1n})e^{-\eta_n x_2}, \quad n = 1,2,3,4, \tag{18}$$

where K_n and K_{1n} functions of the wavenumber b in the direction of the horizontal coordinate x_1 and ω is the complex frequency associated with the propagation of the wave. Utilizing Eq. (18) into Eqs. (10)–(11), a relation below is achieved:

$$\begin{aligned} &K_{1n} = H_{1n}K_n, \\ &H_{1n} = (G_{13}\eta_n^2 + mG_{24}\eta_n - b^2 - g1 - (2\rho\Omega\omega - iG_{12}b\eta_n - mbiG_{26}), \\ &(G_{15}\eta_n^2 - G_{13}b^2 + mG_{27}\eta_n - g1 + (2\rho\Omega\omega + iG_{12}b\eta_n + mbiG_{24}), n = 1,2,3,4. \end{aligned} \tag{19}$$

Thus, the complete solutions of the displacements and stresses utilized for the model problem follows:

$$\begin{aligned} &u_1 = K_n e^{-\eta_n x_2 + \omega t + ibx_1}; u_2 = H_{1n}K_n e^{-\eta_n x_2 + \omega t + ibx_1}, \\ &\sigma_{11} = \left\{ib\left(1 - \left(\frac{\mu_0 H_0^2}{G_1}\right)\right) - \eta_n H_{1n} G_{16}\right\} K_n e^{-(\eta_n + m)x_2 + \omega t + ibx_1}, \\ &\sigma_{22} = \{ibG_{16} - \eta_n H_{1n} G_{17}\} K_n e^{-(\eta_n + m)x_2 + \omega t + ibx_1}, \\ &\sigma_{12} = (ibH_{1n} - \eta_n) G_{13} K_n e^{-(\eta_n + m)x_2 + \omega t + ibx_1}, \\ &\sigma_{21} = G_{13}(ibH_{1n} - \eta_n) K_n e^{-(\eta_n + m)x_2 + \omega t + ibx_1}, n = 1,2,3,4. \end{aligned} \tag{20}$$

Impedance-corrugated conditions of the half-space and dispersions of Rayleigh waves

This section is anchored on formulations and derivations associated with the impedance and corrugated conditions through which dispersion of Rayleigh wave on the fiber-reinforced half-space is explored. Following Asano [5], the corrugated boundary in trigonometric Fourier series denoted $x_2 = \xi(x_1)$ is such that$\xi(x_1) = \xi_l e^{ilbx_1} + \xi_{-l} e^{-ilbx_1}$, $l = 1,2,3,4, \ldots$, where ξ_l and ξ_{-l} gives the Fourier expansion coefficients and l is the series expansion order. Asano represented the parameters a, F_l and I_l in the form $\xi_1^{\pm} = \frac{a}{2}$, $\xi_l^{\pm} = \frac{F_l + I_l}{2}, l = 2,3 \ldots$, such that $\xi(x_1) = a\,cos\,b\,x_1 + F_2\,cos\,2\,bx_1 + I_2\,sin\,2\,bx_1 + \cdots + +F_l\,cos\,l\,bx_1 + I_l\,sin\,l\,bx_1$; F_l and I_l gives the Fourier cosine and sine Fourier coefficients, respectively, and through which the corrugated boundary surface in cosine terms by Asano become $\xi(x_1) = a\,cos\,b\,x_1$. a denote the constant amplitude of the corrugation and b is wavenumber such that $2\pi/b$ gives the wavelength. However, we are interested in variable amplitudes of corrugation of the boundary of the material such that the wavelength of the wave for the corrugated surface equal π/b. This is actually half of the wavelength for a non-variable or uniform amplitude of the wave as given by Asano [5]. For this to occur, we need to redefine the amplitude of the corrugated surface such that $\bar{\xi}_1^{\pm} = (a + cx_1)/2$, and $\bar{\xi}(x_1) = \bar{\xi}_l e^{ilbx_1} + \bar{\xi}_{-l} e^{-ilbx_1}$, $l = 1,2,3,4, \ldots$, through which we can obtain $\bar{\xi}(x_1) = (a + cx_1)\,cos\,b\,x_1 + F_2\,cos\,2\,bx_1 + I_2\,sin\,2\,bx_1 + \ldots + F_l\,cos\,l\,bx_1 + I_l\,sin\,l\,bx_1$.

Here, $\bar{\xi}_l^{\pm} = (F_l + I_l)/2, l = 2,3 \ldots$ Subsequently, we then assume the corrugated

surface boundary to be in the form of cosine term $\bar{\xi}(x_1) = (a + cx_1)\, cos\, b\, x_1$. Here, $(a + cx_1)$ become the variable amplitudes of the corrugated surface and $b$the wave number. Also, a, c are terms associated with amplitudes such that if $c = 0$, we recover the amplitude associated with Asano [5] model. To visualize these scenarios and its geometry, we illustrate $\xi(x_1) = a\, cos\, b\, x_1$ with uniform or constant amplitude of corrugation; $\bar{\xi}(x_1) = (a + cx_1)\, cos\, b\, x_1$ and its derivative – $\bar{\xi}'_1 \, sin\, b_1 \, cos\, b_1$ with variable amplitudes of corrugation graphically in Fig. 1, respectively:

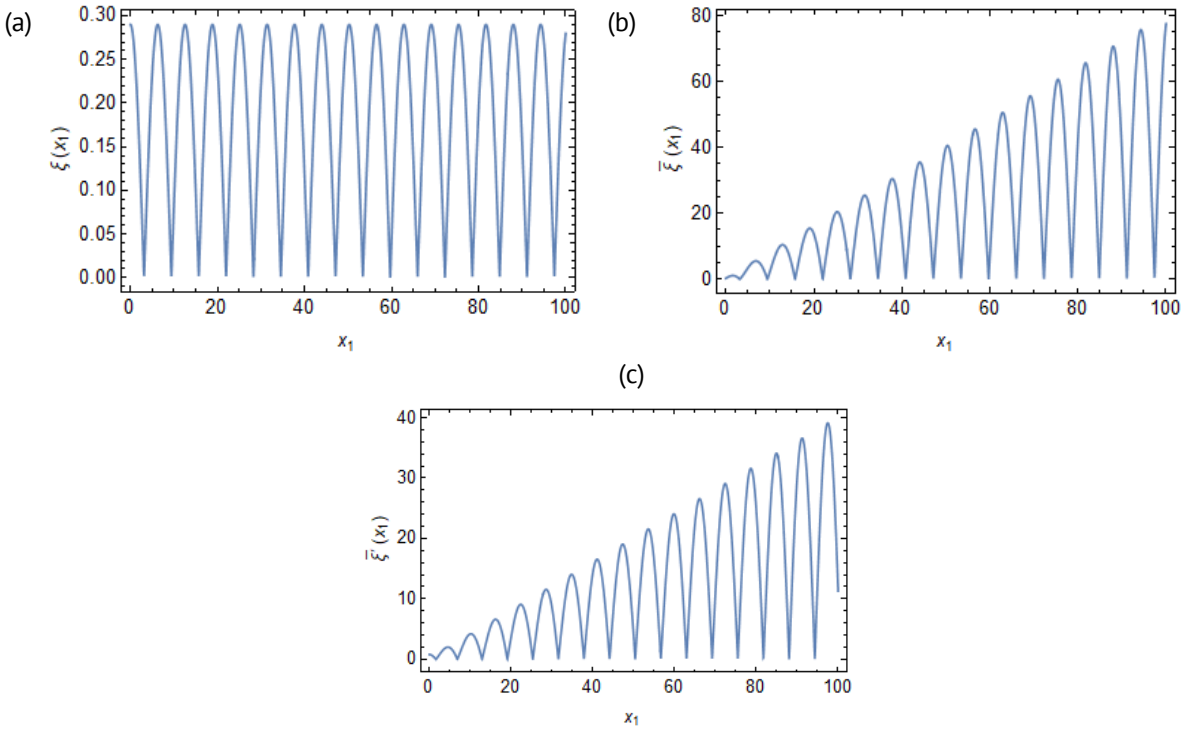

Fig. 1. (a) Uniform amplitude of corrugation; (b) variable amplitude of corrugation; (c) Rate of change of (b) with respect to x_1

(a) Homogenous boundary conditions on the impedance, considering corrugated fibre-reinforced inhomogeneous material: $u_1 = 0$, $u_2 = 0$, at $x_2 = \bar{\xi}(x_1)$, for all x_1 coordinate and at any time t. Conditions on stresses w.r.t $x_2 = \bar{\xi}(x_1)$ gives the following: $\sigma_{22} - \bar{\xi}'(x_1)\sigma_{21} + \bar{\sigma}_{22} + \omega Z_2 u_2 = 0$, that is $\sigma_{22} + \bar{\sigma}_{22} - \bar{\xi}'(x_1)\sigma_{21} + \omega Z_2 u_2 = 0$, $\sigma_{22} + \mu_0 H_0^2\left(u_{1,1} + u_{2,2}\right) - \bar{\xi}'(x_1)\sigma_{21} + \omega Z_2 u_2 = 0$, where $\bar{\sigma}_{22} = \mu_0 H_0^2\left(u_{1,1} + u_{2,2}\right)$, gives Maxwell's additional stress on the fibre-reinforced inhomogeneous material, Abd-Alla et al. [2], Anya et al. [35,36] and Azhar et al. [39]. The tangential stress condition or shear stress follows: $\sigma_{12} - \bar{\xi}'(x_1)\sigma_{11} + \omega Z_1 u_1 = 0$ for all x_1 coordinate and at any time t.

(b) Inhomogeneous boundary conditions on the impedance, considering corrugated fibre-reinforced inhomogeneous material: $u_1 = 0$, $u_2 = 0$, at $x_2 = \bar{\xi}(x_1)$, for all x_1 coordinate and at any time t. Conditions on stresses w.r.t $x_2 = \bar{\xi}(x_1)$ gives the following:
$\sigma_{22} - \bar{\xi}'(x_1)\sigma_{21} + \bar{\sigma}_{22} + \omega Z_2 u_2 = 0$ that is $\sigma_{22} + \bar{\sigma}_{22} - \bar{\xi}'(x_1)\sigma_{21} + \omega Z_2 u_2 = 0$,
$\sigma_{22} + \mu_0 H_0^2(u_{1,1} + u_{2,2}) - \bar{\xi}'(x_1)\sigma_{21} + \omega Z_2 u_2 = 0$, where $\bar{\sigma}_{22} = \mu_0 H_0^2(u_{1,1} + u_{2,2})$, gives Maxwell's additional stress on the fibre-reinforced inhomogeneous material, Abd-Alla et al. [2], Anya et al. [35,36] and Azhar et al. [39]. The tangential stress condition or shear stress

follows: $\sigma_{12} - \bar{\xi}'(x_1)\sigma_{11} + \omega Z_1 u_1 = 0$ for all x_1 coordinate and at any time t. In (b) above, $\bar{Z}_1$ and $\bar{Z}_2$ are the impedance parameters, Anya et al. [35,36] and Ailawalia et al. [40]. We assume that these impedance parameters $\bar{Z}_1$ and $\bar{Z}_2$ are inhomogeneous. This is such that $(\bar{Z}_1, \bar{Z}_2) = (Z_1, Z_2)e^{-mx_2}$. But note that Z_1, Z_2 are homogeneous at the boundary of (a). Hence, these assumptions imply the following two sets of four equations from (a) and (b) above, respectively. They are presented below as (c) and (d), respectively.

(c) Homogenous boundary conditions on the impedance considering fiber-reinforced inhomogeneous material:

$$K_n = 0, \tag{21}$$

$$H_{1n}K_n = 0, \tag{22}$$

$$\{ibG_{16} - \eta_n H_{1n}G_{17}\}e^{-(\eta_n+m)\bar{\xi}(x_1)}K_n + [(a+cx_1)b\sin b\,x_1 - c\cos b\,x_1]\{(ibH_{1n} - -\eta_n)G_{13}\} \times\times e^{-(\eta_n+m)\bar{\xi}(x_1)}K_n + \{\mu_0 H_0^2(ib - \eta_n H_{1n})\}e^{-(\eta_n+m)\bar{\xi}(x_1)}K_n + +\{\omega H_{1n}Z_2K_n\} = 0, \tag{23}$$

$$\left\{\{ibH_{1n} - \eta_n\}G_{13} + [(a+cx_1)b\sin b\,x_1 - c\cos b\,x_1]\{ib\left(1 - (\mu_0 H_0^2/G_1)\right) - -\eta_n H_{1n}G_{16}\}\right\} \times K_n e^{-(\eta_n+m)\bar{\xi}(x_1)} + \{\omega Z_1\}K_n = 0. \tag{24}$$

(d) Inhomogenous boundary conditions on the impedance considering fiber-reinforced inhomogeneous material:

$$K_n = 0, \tag{25}$$

$$H_{1n}K_n = 0, \tag{26}$$

$$\{ibG_{16} - \eta_n H_{1n}G_{17}\}e^{-\eta_n\bar{\xi}(x_1)}K_n + [(a+cx_1)b\sin b\,x_1 - c\cos b\,x_1]\{(ibH_{1n} - -\eta_n)G_{13}\}e^{-\eta_n\bar{\xi}(x_1)}K_n + \{\omega H_{1n}Z_2K_n + \mu_0 H_0^2(ib - \eta_n H_{1n})\}e^{-\eta_n\bar{\xi}(x_1)}K_n = 0, \tag{27}$$

$$\{\{ibH_{1n} - \eta_n\}G_{13}K_n + [(a+cx_1)b\sin b\,x_1 - c\cos b\,x_1]\{ib(1 - (\mu_0 H_0^2/G_1)) - -\eta_n H_{1n}G_{16}\}K_n + \{\omega Z_1\}\}K_n e^{-\eta_n\bar{\xi}(x_1)} = 0, \quad n = 1,2,3,4. \tag{28}$$

For non-trivial solutions in (a) and (b), the determinants $|K_{ij}| = 0, \quad i = j = 1,2,3,4$ and for $K_n \neq 0$, gives the novel respective two dispersion relations $|\nabla|$ of the Rayleigh wave for: (a) homogeneous conditions on the impedance and (b) inhomogeneous conditions on the impedance.

Computational results and Discussion

This section devotes wholly on depicting our analytical solution graphically. To achieve this, we employ the numerical fiber-reinforced constants as given by Othman et al. [41] and some other parameters below to demonstrate the variations or effects of the physical quantities of impedance, rotation, inhomogeneity, magnetic fields, variable amplitudes of corrugated parameters and the wavenumber on the two dispersions of Rayleigh wave considering when the impedance applied on the material is homogeneous and when the impedance applied is inhomogeneous. It should be noted that the fiber-reinforced solid half-space is inhomogeneous: $\lambda = 7.59 \cdot 10^9$ kg m^{-1}s^{-2}, $\mu_L = 2.45 \cdot 10^9$ kg m^{-1}s^{-2}, $\mu_T = 1.89 \cdot 10^9$ kg m^{-1}s^{-2}, $\rho = 7.8 \cdot 10^3$ kg m^{-3}, $\alpha = -1.28 \cdot 10^9$ kg m^{-1}s^{-2}, $\beta = 0.32 \cdot 10^9$ kg m^{-1}s^{-2}, $\omega = (0.02 + \mathrm{i})$ rad/s, $a = 0.29$.

Figure 2 entails the variation of magnetic field H_0 on the dispersions $|\nabla|$ of Rayleigh wave as against x_1 coordinate, considering (a) homogeneous impedance and (b) inhomogeneous impedance on an inhomogeneous solid half-space such that all other physical parameters of impedance Z_i, $i = 1,2$, rotation Ω of the medium,

inhomogeneity$m$, corrugated parameters (a, c and b) i.e. parameters linked with the variable amplitudes of corrugation and wavenumber, respectively, are assumed to be in fixed state on the inhomogeneous fiber-reinforced solid half-space. Hence, increase in the magnetic field H_0 results to a corresponding increase in the behavior of the dispersions $|\nabla|$. In fact, the minima amplitudes of the dispersions $|\nabla|$ are attained when we neglect the magnetic field on the material. While the maxima amplitudes of the dispersions $|\nabla|$ are attained at $x_1 = 0.7$ and $x_1 = 0.6$ for an increasing magnetic field H_0 application especially on Fig. 2(a) and Fig. 2(b), respectively. Also, we observe that the dispersion relations $|\nabla|$ decrease for an extended x_1 coordinate such that the behavior of the dispersions $|\nabla|$ due to (a) homogeneous impedance and (b) inhomogeneous impedance on an inhomogeneous solid half-space are alike in every aspect except in their respective dispersion amplitudes and a difference in behavior when $x_1 \geq 1.4$. Physically, this has shown that the presence of external magnetic field influences the wave propagation especially as a push to the material characterizations and thus, impacts the wave attenuation and velocity of propagation. Hence, low magnetic fields on the model tend to give reduced influences of propagation as observed.

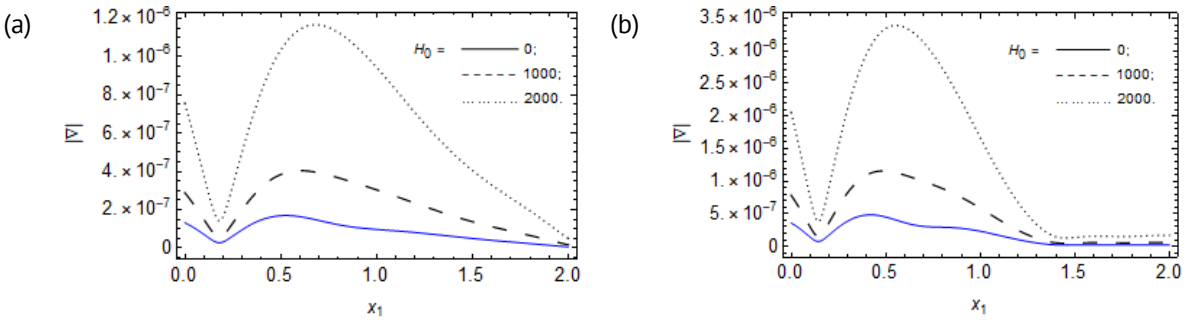

Fig 2. Variation of magnetic field $H_0(A/m)$ on the dispersions $|\nabla|$ of Rayleigh wave against x_1, considering (a) homogeneous impedance; (b) inhomogeneous impedance on an Inhomogeneous solid half-space

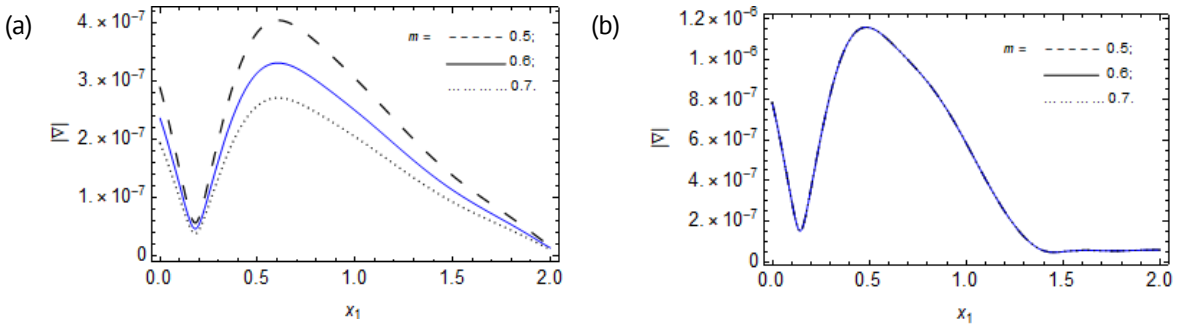

Fig. 3. Variation of inhomogeneous parameter m on the dispersions $|\nabla|$ of Rayleigh wave against x_1, considering (a) homogeneous impedance and (b) inhomogeneous impedance on an Inhomogeneous solid half-space

Consequently, Fig. 3 demonstrates the effect of the inhomogeneous parameter $m$on the dispersions $|\nabla|$ of Rayleigh wave against$x_1$coordinate, considering (a) homogeneous impedance and (b) inhomogeneous impedance on an inhomogeneous solid half-space through a constant applications of the physical quantities of magnetic field H_0, impedance $Z_i,\ i = 1,2$, rotation Ω of the medium, corrugated parameters (a, c and b) i.e. parameters associated with the variable amplitudes of corrugation and wavenumber, respectively, on the material.

This is such that an increase in the inhomogeneity m result to a sequential decrease in behavior of the dispersion relation $|\nabla|$ of the wave due to homogeneous impedance that is Fig. 3(a) while the dispersion $|\nabla|$ due to inhomogeneous impedance; Fig. 3(b) possess negligible behavior. That is, the minima value of dispersion due to the homogeneous impedance is attained when the inhomogeneity m increase. However, both considerations; Fig. 3(a) and Fig. 3(b) attain their maxima values of dispersions $|\nabla|$close to $x_1 = 0.6$ and $x_1 = 0.5$, respectively. For extended length of the material both dispersions decreases whilst noticing a difference in behavior for $x_1 \geq 1.4$ and the short dispersion amplitudes of the Rayleigh wave due to homogeneous impedance as compared with the dispersion amplitudes of the Rayleigh wave due to inhomogeneous impedance. This could be physically attributed to the characterizations of the solid half-space owing to fiber-reinforcement, homogeneous impedance and inhomogeneous impedance considerations on the inhomogeneous fiber-reinforced. Thus, it suffices to infer that the impact of the wave velocity and attenuation on the homogeneous characterization of the material would be pronounced as compared with the inhomogeneous material for the considered same physical parameters of the model.

More so, Fig. 4 depicts the effect of rotation Ω of the medium on the dispersions$|\nabla|$ of Rayleigh wave against x_1 coordinate, considering (a) homogeneous impedance and (b) inhomogeneous impedance on an inhomogeneous solid half-space especially when the quantities of magnetic field H_0, impedance Z_i, $i = 1{,}2$, inhomogeneous parameter m, corrugated parameters (a, c) i.e. parameters associated with the variable amplitudes of corrugation and wavenumber b are unchanged on the solid half-space.

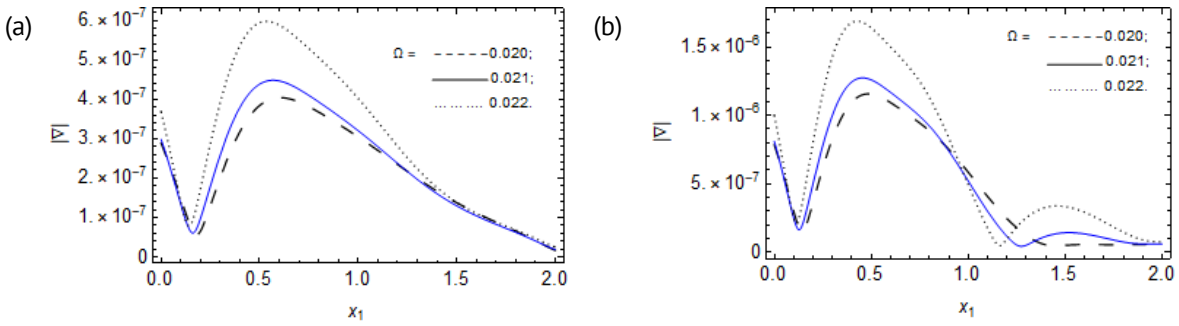

Fig. 4. Variation of rotation Ω, rad/s on the dispersions $|\nabla|$ of Rayleigh wave against x_1, considering (a) homogeneous impedance and (b) inhomogeneous impedance on an Inhomogeneous solid half-space

We observe that both conditions possess mixed behaviors in some domains of the Rayleigh wave dispersion profile when the rotation increase. That is, the two dispersions tend to move in upward trend for an increase in rotation within the domain $0 \leq x_1 < 1$ whilst possessing mixed behavior (increase and decrease) and after which the increase ensues again in a minimal manner, sequentially. However, for an increase in rotation, an outright decrease in behavior equally occur within the domain $0.95 < x_1 < 1.25$ in Fig. 3(b). Near $x_1 = 0.55$ and $x_1 = 0.45$ gives the positions of the maxima values of the dispersions of the Rayleigh wave on the material for Fig. 3(a) and Fig. 3(b), respectively. Hence, we can infer that the maxima values occur when the rotation is large on the material. And again, the amplitude of the dispersion due to inhomogeneous impedance is large as compared with the amplitude of the dispersion due to homogeneous

impedance, i.e., both has very close behavior aside their amplitudes and the behavior around the extended length of the material say from $x_1 > 1.4$. Realistically and across the length of the material, it is evident that the wave modulation is being impacted by rotation of the medium in a higher proportion.

Nevertheless, Fig. 5 connotes the impact of a associated with the variable amplitude of corrugation on the dispersions $|\nabla|$ of Rayleigh wave as against x_1 coordinate, considering (a) homogeneous impedance and (b) inhomogeneous impedance on the inhomogeneous medium. This is feasible only on the constant application of the physical parameters of rotation Ω, magnetic field H_0, impedance Z_i, $i = 1,2$, inhomogeneous parameter m, corrugated parameter c (parameter associated with the variable amplitudes of corrugation) and wavenumber $b$on the inhomogeneous solid half-space. Following this, Fig. 5(a) and Fig. 5(b) decrease sequentially in the domains $0.5 < x_1 \leq 2$ and $0.6 < x_1 \leq 1.1$, respectively when the parameter a associated with the variable amplitude of corrugation increase. We equally note mix behavior in both cases in the domain $0 < x_1 \leq 0.1$. Fig. 5(b) increases again for an increase in a from $x_1 > 1.3$ before mix behavior ensued. More so, the maxima profiles of the dispersions in Fig. 5(a) and Fig. 5(b) of the Rayleigh wave were attain close to $x_1 = 0.35$ and $x_1 = 0.3$, respectively, especially when a associated with the variable amplitude of corrugation increase. Generally, the dispersions of the wave tend to decrease along the length of the material as the wave propagate. We note that both cases have differences in dispersion amplitudes on the considered length of the solid medium and as well as in behaviors for extended length of the material.

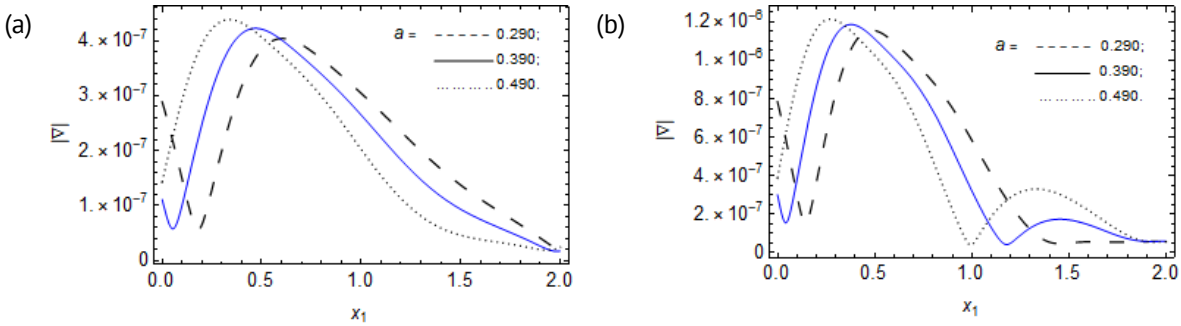

Fig. 5. Variation of a associated with the variable amplitude of corrugation on the dispersions $|\nabla|$ of Rayleigh wave against x_1, considering (a) homogeneous impedance and (b) inhomogeneous impedance on an Inhomogeneous solid half-space

In a similar analysis, Fig. 6 demonstrates the effect of c associated with the variable amplitude of corrugation on the dispersions $|\nabla|$ of Rayleigh wave as against x_1 coordinate, considering (a) homogeneous impedance and (b) inhomogeneous impedance on the inhomogeneous medium. This is such that the physical parameters of rotation Ω, magnetic field H_0, impedance Z_i, $i = 1,2$, inhomogeneous parameter m, corrugated parameter a (parameter associated with the variable amplitudes of corrugation) and wavenumber b remain steady on the material. Hence, we note that parameter c associated with the variable amplitude of corrugation gradually increase the dispersions of the Rayleigh wave when increased in both cases especially within the domain $0 < x_1 \leq 0.8$ for Fig. 6(a) and $0 < x_1 \leq 1.4$ for Fig. 6(b), and after which a very gradual decrease and

a uniform behavior, respectively, occurs. In addition, for the dispersion due to homogeneous impedance, the parameter $c$decrease the dispersion relations of the Rayleigh wave in the domain $0.8 < x_1 \leq 2$ when increased whilst observing uniform behavior for the inhomogeneous impedance case when $x_1 > 1.4$. More so, for an increase in c associated with the variable amplitude of corrugation, the maxima profiles of the dispersions of the Rayleigh wave were recorded close to $x_1 = 0.49$. Thus, we can deduce that the dispersions of the wave tend to decrease along the length of the material as the wave propagate whilst noting that both cases have differences in dispersion profiles in terms of their amplitudes and behaviors at the extended length of the coordinate.

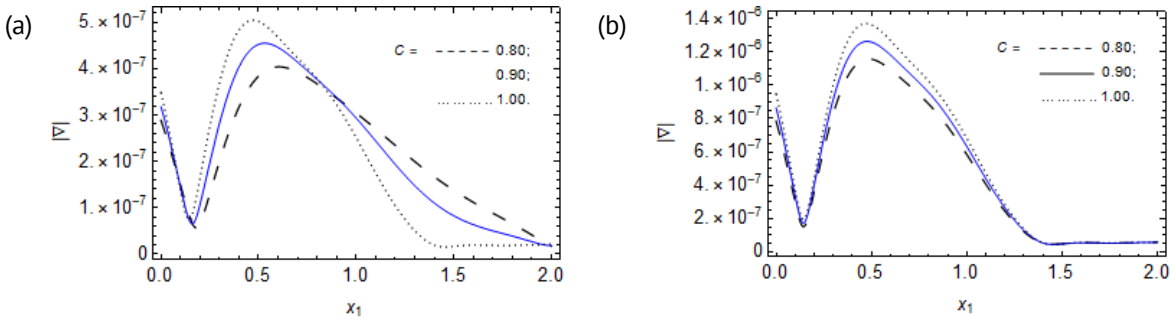

Fig. 6. Variation of c associated with the variable amplitude of corrugation on the dispersions $|\nabla|$ of Rayleigh wave against x_1, considering (a) homogeneous impedance and (b) inhomogeneous impedance on an Inhomogeneous solid half-space

Be that as it may, Fig. 7 depicts the impact of the wavenumber b (associated with the corrugation) on the dispersions $|\nabla|$ of Rayleigh wave as against x_1 coordinate, considering (a) homogeneous impedance and (b) inhomogeneous impedance on the inhomogeneous medium when the parameters of rotation Ω, magnetic field H_0, impedance Z_i, $i = 1{,}2$, inhomogeneous parameter m, corrugated parameters (a, c) (parameters associated with the variable amplitudes of corrugation) are in fixed state on the medium.

We deduce that the dispersion profiles of the Rayleigh wave in both cases show some outright mixed behaviors (uniform, decrease and increase) in certain domains of the horizontal coordinate x_1 when the wavenumber b increase. However, an outright downward trend ensues in the domain $0.5 < x_1 \leq 1.8$ in Fig. 7(b) when the wavenumber

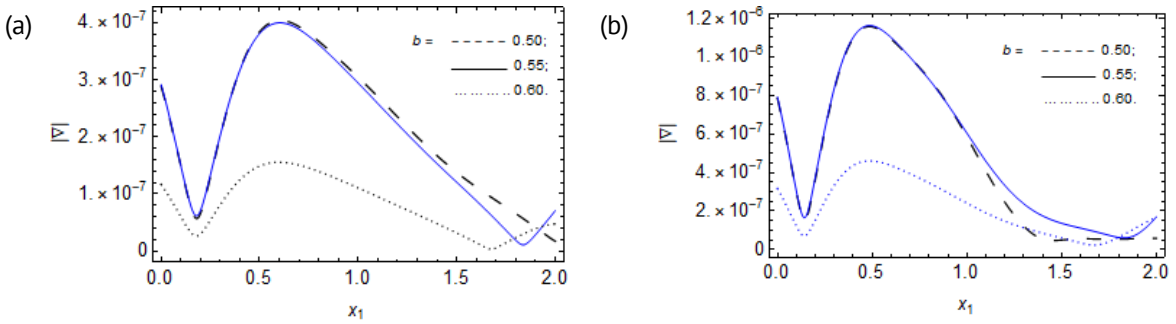

Fig. 7. Variation of wavenumber b associated with the corrugation on the dispersions $|\nabla|$ of Rayleigh wave against x_1, considering (a) homogeneous impedance and (b) inhomogeneous impedance on an Inhomogeneous solid half-space

b increase. The maxima values in Fig. 7(a) and Fig. 7 (b) occur near $x_1 = 0.6$ and $x_1 = 0.5$, respectively while the minima values of the dispersions occur when b is large. When $b = 0.5$ and along the extended length of the material, there exist gradual upward trend different from the initial behavior of the dispersions. We equally observe as in Fig. 6, that Fig. 7 possess reduce amplitude of dispersion for the dispersion due to homogeneous impedance as compared with the amplitude of dispersion occasioned by the inhomogeneous impedance. This can be attributed to the homogeneous impedance and inhomogeneous impedance considerations on the inhomogeneous fiber-reinforced solid. Thus, owing to the considered geometry, it is inferred that the number of cycles or wavelengths per unit of distance (wave number) has huge influence on the wave propagation on the material such that mixed occurrences of the Rayleigh wave were recorded across certain positions on the material.

In a different vein, Fig. 8 depicts the effect of impedance Z_2 on the dispersions$|\nabla|$of Rayleigh wave as against$x_1$coordinate, considering (a) homogeneous impedance and (b) inhomogeneous impedance on the inhomogeneous medium when the parameters of wavenumber b, rotation Ω, magnetic field H_0, impedance Z_i, $i = 1$, inhomogeneous parameter$m$, corrugated parameters (a, c) (parameters associated with the variable amplitudes of corrugation) are unchanged on the solid medium. Figure 8 shows that increase in the impedance Z_2 yield negligible behavior in terms of increase and decrease on both considered dispersions of Fig. 8(a) and Fig. 8(b), respectively. However, they dispersions in both cases are uniformly distributed in this instance of increase in Z_2. They attain maxima values close to $x_1 = 0.6$ and $x_1 = 0.5$, respectively at any of the given Z_2. This can be attributed to the material exhibition where the resistant-like phenomena of the impedance is felt or witnessed. However, Fig. 8(a) has a reduced dispersion amplitude as compared with Fig. 8(b). This can be attributed to the homogeneous impedance and inhomogeneous impedance considerations on the inhomogeneous fiber-reinforced medium.

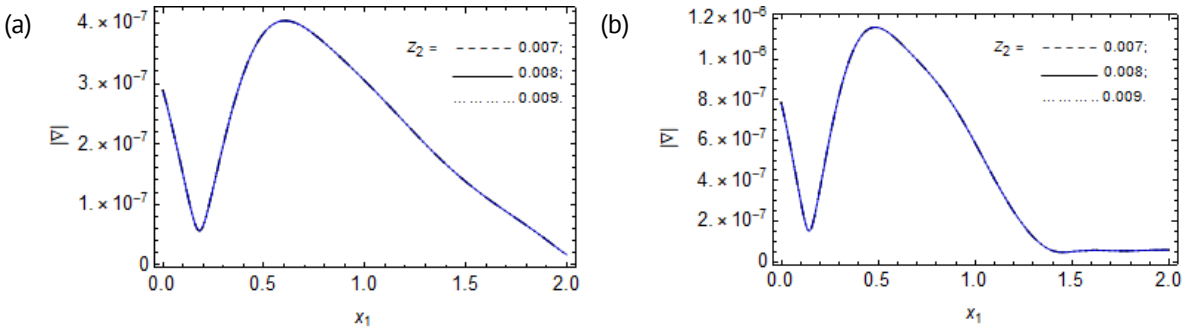

Fig. 8. Variation of impedance Z_2 on the dispersions $|\nabla|$ of Rayleigh wave against x_1, considering (a) homogeneous impedance and (b) inhomogeneous impedance on an Inhomogeneous solid half-space

In a similar vein, Fig. 9 demonstrates the effect of impedance Z_1 on the dispersions$|\nabla|$ of Rayleigh wave as against x_1 coordinate, considering (a) homogeneous impedance and (b) inhomogeneous impedance on the inhomogeneous medium when the parameters of wavenumber b, rotation Ω, magnetic field H_0, impedance Z_i, $i = 2$, inhomogeneous parameter m, parameters associated with the variable amplitudes of corrugation (a, c) remain constantly applied on the solid. In the light of this, Fig. 9 shows

that increase in the impedance Z_1 yield negligible behavior on both considered dispersions of (a) and (b), respectively in terms of decrease an increase. They attain maxima values close to $x_1 = 0.6$ and $x_1 = 0.5$, respectively at any of the given Z_1. This can be attributed to the material characteristics where a resistant-like phenomena of the impedance is witnessed. However, Fig. 9(a) has a reduced dispersion amplitude as compared with Fig. 9(b). This can be attributed to the homogeneous impedance and inhomogeneous impedance considerations on the inhomogeneous fiber-reinforced medium. We can say that this analysis on Z_1 is alike to analysis on Fig. 8 with uniform distributed dispersions at this instance.

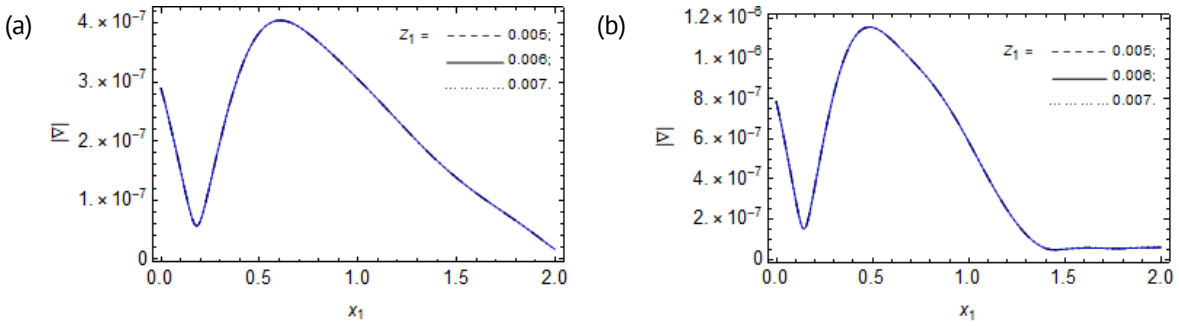

Fig. 9. Variation of impedance Z_1 on the dispersions $|\nabla|$ of Rayleigh wave against x_1, considering (a) homogeneous impedance and (b) inhomogeneous impedance on an Inhomogeneous solid half-space

Conclusions

The present investigation aimed at exploring a mathematical model and its analysis, occasioned by the dispersion relation of Rayleigh wave in a rotating inhomogeneous half-space with variable corrugation amplitudes and impedance conditions under magnetic influence. The impedance conditions were made to be in two characterizations i.e., homogeneous impedance and inhomogeneous impedance conditions at the boundary of the material. We employed the constitutive relations for a fiber-reinforced material alongside an exponentially decaying function of the material parameters characterizing the inhomogeneity, rotation of the medium and magnetism in deriving the equations of motion of the wave on the material. Through this, the analytical solution of the model was derived using the normal mode analysis. Subsequently, using the corrugated-impedance boundary conditions, the two dispersion relations of Rayleigh wave for homogeneous impedance and inhomogeneous impedance conditions were formulated. The graphical depictions of these two dispersion relations of Rayleigh wave where the variations of the physical parameters of rotation, inhomogeneity, magnetic field, impedance, wavenumber and variable amplitudes of corrugation parameters were carried out are illustrated. This is such that:

1. An increase in the magnetic field H_0 give rise to increase in the behavior for the two dispersion relations of the Rayleigh wave on the inhomogeneous fiber-reinforced medium, that is, dispersion due to inhomogeneous impedance and dispersion due to homogeneous impedance increases for increase in H_0.
2. Increase in the inhomogeneity m result to a sequential decrease in behavior of the dispersion relation of the wave due to homogeneous impedance while the dispersion due

to inhomogeneous impedance possesses negligible behavior at this instance.
3. A larger portion of the dispersion profiles witnessed increase in behavior when the rotation Ω increase. However, the rotation Ω of the medium yielded mix behaviors on the dispersion relation of the Rayleigh wave especially in certain domains of the horizontal coordinate when increased.
4. The parameter a associated with the variable amplitude of corrugation caused both decreasing behavior and increasing behavior on both dispersion relations of the wave in certain domains of the horizontal coordinate especially when increased. While the parameter c which is also associated with the variable amplitude of corrugation caused an upward trend on both dispersion relations of the Rayleigh wave when increased. This occurrence ensued especially to a larger extent in the domain of the horizontal coordinate where a very slight mix behavior occurs afterwards. In addition, for the dispersion due to homogeneous impedance, the parameter $c$decrease the dispersion relations of the Rayleigh wave in the domain $0.8 < x_1 \leq 2$ when increased whilst observing uniform behavior for the inhomogeneous impedance case when $x_1 > 1.4$.
5. The wavenumber associated with the variable corrugated surfaces tend to cause a decrease in behavior to the dispersions of the waves to a large extent when increased while noting some mixed behaviors in both cases towards the extended part of the material.
6. Impedance parameters, that is, both the normal and horizontal impedances behaved alike such that they pulled a resistant-like measure on the material by exhibiting a negligible impact when increased on the material in terms of increase and decrease. However, we can equally adduce that the dispersions in both cases were uniformly distributed in this instance.

Thus, it is imperative to state that this model and its analysis invoke special cases found in the literature when the variable amplitude parameter $c$is neglected, i.e., at $c = 0$, models related to Asano [4] are gotten for constant or uniform amplitude of corrugation as occasioned in Fig. 1(a). Hence, we adduce that this study should be beneficial to the investigation and characterization of new and old materials, mathematics of wave phenomena cum solution, and the entire research community working in the directions similar to surface waves on solid materials. Also, the most immediate and realistic engineering applications where the joint interactions of Rayleigh wave, magnetic influences, rotation and fiber reinforcement becomes eminent or applicable is in the design and failure analysis of rotating machinery components designed from composite materials, like those in aerospace materials especially in rotor blades, non-destructive testing using surface waves, and making of piezo-magneto-electric sensors and actuator technologies.

CRediT authorship contribution statement

Augustine I. Anya : conceptualization, methodology, investigation, writing – review & editing, writing – original draft, data curation.

Conflict of interest

The author declares that there is no conflict of interest.

References

1. Spencer AJM. *Deformations of fiber-reinforced materials*. Oxford: Oxford University Press; 1972.
2. Abd-Alla AM, Abo-Dahab SM, Khan A. Rotational effects on magneto-thermoelastic Stonely, Love, and Rayleigh waves in fiber-reinforced anisotropic general viscoelastic media of higher order. *CMC – Computers, Materials & Continua.* 2017;53(1): 49–72.
3. Schoenberg M, Censor D. Elastic waves in rotating media. *Quarterly of Applied Mathematics.* 1973;15: 115–125.
4. Singh B. Reflection of Elastic Waves from Plane Surface of a Half-space with Impedance Boundary Conditions. *Geosciences Research.* 2017;2(4): 242–253.
5. Asano S. Reflection and refraction of elastic waves at a corrugated interface. *Bulletin of the Seismological Society of America.* 1966;56(1): 201–221.
6. Singh SS, Tomar SK. qP-wave at a corrugated interface between two dissimilar pre-stressed elastic half-spaces. *Journal of Sound and Vibration.* 2008;317(3–5): 687–708.
7. Singh AK, Das A, Kumar S, Chattopadhyay A. Influence of corrugated boundary surfaces, reinforcement, hydrostatic stress, heterogeneity and anisotropy on Love-type wave propagation. *Meccanica.* 2015;50: 2977–2994.
8. Singh AK, Mistri KC, Pal MK. Effect of loose bonding and corrugated boundary surface on propagation of Rayleigh-type wave. *Latin American Journal of Solids and Structures.* 2018;15(1): e01.
9. Das SC, Acharya DP, Sengupta PR. Surface waves in an inhomogeneous elastic medium under the influence of gravity. *Romanian Journal of Technical Sciences. Applied Mechanics.* 1992;37(5): 539–551.
10. Abd-Alla AM, Abo-Dahab SM, Alotaibi HA. Effect of the rotation on a non-homogeneous infinite elastic cylinder of orthotropic material with magnetic field. *Journal of Computational and Theoretical Nanoscience.* 2016;13(7): 4476–4492.
11. Chattopadhyay A. On the dispersion equation for Love waves due to irregularity in the thickness of the non-homogeneous crustal layer. *Acta Geologica Polonica.* 1975;23: 307–317.
12. Roy I, Acharya DP, Acharya S. Propagation and reflection of plane waves in a rotating magneto-elastic fiber-reinforced semi-space with surface stress. *Mechanics and Mechanical Engineering.* 2018;22(4): 939–957.
13. Singh D, Sindhu R. Propagation of waves at an interface between a liquid half-space and an orthotropic micropolar solid half-space. *Advances in Acoustics and Vibration.* 2011;2011(1): 159437.
14. Gupta RR. Surface wave characteristics in a micropolar transversely isotropic half-space underlying an inviscid liquid layer. *International Journal of Applied Mechanics and Engineering.* 2014;19(1): 49–60.
15. Anya AI, Akhtar MW, Abo-Dahab SM, Kaneez H, Khan A, Jahangir A. Effects of a magnetic field and initial stress on reflection of SV-waves at a free surface with voids under gravity. *Journal of the Mechanical Behavior of Materials.* 2018;27(5–6): 20180002.
16. Anya AI, Khan A. Reflection and propagation of plane waves at free surfaces of a rotating micropolar fiber-reinforced medium with voids. *Geomechanics and Engineering.* 2019;18(6):605–614.
17. Anya AI, Khan A. Reflection and propagation of magneto-thermoelastic plane waves at free surfaces of a rotating micropolar fiber-reinforced medium under GL theory. *International Journal of Acoustics and Vibration.* 2020;25(2): 190–199.
18. Anya AI, Khan A. Plane waves in a micropolar fiber-reinforced solid and liquid interface for non-insulated boundary under magneto-thermo-elasticity. *Journal of Computational Applied Mechanics.* 2022;53(2): 204–218.
19. Maleki F, Jafarzadeh F. Model tests on determining the effect of various geometrical aspects on horizontal impedance function of surface footings. To be published in *Scientia Iranica.* [Preprint] 2023. Available from: doi.org/10.24200/SCI.2023.59744.6403.
20. Chowdhury S, Kundu S, Alam P, Gupta S. Dispersion of Stoneley waves through the irregular common interface of two hydrostatic stressed MTI media. *Scientia Iranica.* 2021;28(2): 837–846.
21. Singh B, Kaur B. Rayleigh surface wave at an impedance boundary of an incompressible micropolar solid half-space. *Mechanics of Advanced Materials and Structures.* 2022;29(25): 3942–3949.
22. Singh B, Kaur B. Rayleigh-type surface wave on a rotating orthotropic elastic half-space with impedance boundary conditions. *Journal of Vibration and Control.* 2020;26(21–22): 1980–1987.
23. Sahu SA, Mondal S, Nirwal S. Mathematical analysis of Rayleigh waves at the nonplanner boundary

between orthotropic and micropolar media. *International Journal of Geomechanics.* 2023;23(3): 04022313.
24. Giovannini L. Theory of dipole-exchange spin-wave propagation in periodically corrugated films. *Physical Review B.* 2022;105(21): 214426.
25. Rakshit S, Mistri KC, Das A, Lakshman A. Effect of interfacial imperfections on SH-wave propagation in a porous piezoelectric composite. *Mechanics of Advanced Materials and Structures.* 2022;29(25): 4008–4018.
26. Rakshit S, Mistri KC, Das A, Lakshman A. Stress analysis on the irregular surface of visco-porous piezoelectric half-space subjected to a moving load. *Journal of Intelligent Material Systems and Structures.* 2022;33(10): 1244–1270.
27. Gupta V, Kumar M, Goel Sh. Study of different theories of thermoelasticity under the Rayleigh wave propagation along an isothermal boundary. *Materials Physics and Mechanics.* 2025;53(1): 22–37.
28. Kaushal S, Kumar R, Kochar A. Wave propagation under the influence of voids and non-free surfaces in a micropolar elastic medium. *Materials Physics and Mechanics.* 2022;50(2): 226-238.
29. Sharma S, Batra D, Kumar R. Fractional strain analysis on reflection of plane waves at an impedance boundary of a non-local swelling porous thermoelastic medium. *Materials Physics and Mechanics.* 2025;53(1): 1–21.
30. Sharma JN, Othman MIA. Effect of rotation on generalized thermo-viscoelastic Rayleigh–Lamb waves. *International Journal of Solids and Structures.* 2007;44(13): 4243–4255.
31. Shaw S, Othman MIA. Characteristics of Rayleigh wave propagating in an orthotropic magneto-thermoelastic half-space: An eigen function expansion method. *Applied Mathematical Modelling.* 2019;67: 605–620.
32. Othman MIA, Zidan MEM, Hilal MIM. Effect of magnetic field on a rotating thermoelastic medium with voids under thermal loading due to laser pulse with energy dissipation. *Canadian Journal of Physics.* 2014;92(11): 1359–1371.
33. Othman MIA, Song YQ. The effect of rotation on 2-D thermal shock problems for a generalized magneto-thermoelastic half-space under three theories. *Multidiscipline Modeling in Materials and Structures.* 2009;5(1): 43–58.
34. Othman MIA, Saied SM. The effect of rotation on two-dimensional problem of a fiber-reinforced thermoelastic medium with one relaxation time. *International Journal of Thermophysics.* 2012;33(2): 160–171.
35. Anya AI, Nwachioma C, Ali H. Magnetic effects on surface waves in a rotating non-homogeneous half-space with grooved and impedance boundary characteristics. *International Journal of Applied Mechanics and Engineering.* 2023;28(4): 26–42.
36. Anya AI, Khan A. Propagation and reflection of magneto-elastic plane waves at the free surface of a rotating micropolar fiber-reinforced medium with voids. *Journal of Theoretical and Applied Mechanics.* 2019;57(4): 869–881.
37. Khan A, Anya AI, Kaneez H. Gravitational effects on surface waves in non-homogeneous rotating fiber-reinforced anisotropic elastic media with voids. *International Journal of Applied Science and Engineering Research.* 2015;4: 620–632.
38. Munish S, Sharma A, Sharma A. Propagation of SH waves in double non-homogeneous crustal layers of finite depth lying over a homogeneous half-space. *Latin American Journal of Solids and Structures.* 2016;13(14): 2628–2642.
39. Azhar E, Ali H, Jahangir A, Anya AI. Effect of Hall current on reflection phenomenon of magneto-thermoelastic waves in a non-local semiconducting solid. To be published in *Waves in Random and Complex Media.* [Preprint] 2023. Available from: doi.org/10.1080/17455030.2023.2182146.
40. Ailawalia P, Sachdeva SK, Pathania D. A two dimensional fiber-reinforced micropolar thermoelastic problem for a half-space subjected to mechanical force. *Theoretical and Applied Mechanics.* 2015;42(1): 11–25.
41. Othman MIA, Lofty Kh. The effect of magnetic field and rotation on the 2-D problem of a fiber-reinforced thermoelastic medium under three theories with influence of gravity. *Mechanics of Materials.* 2013;60: 129–143.

Nomenclatures

b is wavenumber;
$a,\ c$ are parameters associated with variable amplitude of corrugation;
σ_{ij} is stress tensor;
ε_{ij} is strain tensor;
u_i is displacement vector;
δ_{ij} is Kronecker-Delta function;
λ is Lame's constant;
α, β, $(\mu_L - \mu_T)$ are fiber-reinforced parameters;

F_i is Magnetic force;
ε_0 is electric permeability;
μ_0 is Magnetic permeability;
H_i is Magnetic vector field;
Ω is Rotation parameter of the medium;
ρ is density;
x_i are coordinates;
$Z_1,\ Z_2$ are impedance parameters.

Appendix

$d_{11} = G_{13}G_{15}$;
$d_{12} = -m(G_{15}G_{24} + G_{13}G_{27})$;
$d_{13} = (-b^2i^2\rho G_{12}^2 - b^2\rho G_{15} - \rho\omega^2 G_{15} + \rho^2\Omega^2 G_{15} + m^2\rho G_{24}G_{27} - \omega^2 G_{15}H_0^2\varepsilon_0\mu_0^2 +$
$+G_{13}(-\rho\omega^2 + \rho^2\Omega^2 - b^2\rho G_{13} - \omega^2 H_0^2\mu_0^2))/\rho$;
$d_{14} = (m(b^2i^2\rho G_{12}G_{26} + G_{24}(\rho\omega^2 - \rho^2\Omega^2 + b^2i^2\rho G_{12} + b^2\rho G_{13} + \omega^2 H_0^2\mu_0^2) +$
$+G_{27}(\rho(b^2 + \omega^2 - \rho\Omega^2) + \omega^2 H_0^2\varepsilon_0\mu_0^2)))/\rho$;
$d_{15} = \frac{1}{\rho^2}(b^2\rho^2\omega^2 + \rho^2\omega^4 - b^2\rho^3\Omega^2 - 2\rho^3\omega^2\Omega^2 + 4\rho^4\omega^2\Omega^2 + \rho^4\Omega^4 - 2bim\rho^3\omega\Omega G_{26} +$
$+bim\rho^2 G_{24}(2\rho\omega\Omega - bimG_{26}) + b^2\rho\omega^2 H_0^2\mu_0^2 + \rho\omega^4 H_0^2\mu_0^2 - \rho^2\omega^2\Omega^2 H_0^2\mu_0^2 + \rho\omega^4 H_0^2\varepsilon_0\mu_0^2 -$
$-\rho^2\omega^2\Omega^2 H_0^2\varepsilon_0\mu_0^2 + \omega^4 H_0^4\varepsilon_0\mu_0^4 + b^2\rho G_{13}(\rho(b^2 + \omega^2 - \rho\Omega^2) + \omega^2 H_0^2\varepsilon_0\mu_0^2))$.